International Journal of Solids and Structures 45 (2008) 4574–4589

Contents lists available at ScienceDirect

International Journal of Solids and Structures

journal homepage: www.elsevier.com/locate/ijsolstr

Analysis of multiple off-axis ply cracks in composite laminates

Chandra Veer Singh *, Ramesh Talreja

Department of Aerospace Engineering, Texas A&M University College Station, TX 77843-3141, USA

ARTICLE INFO

Article history:
Received 21 August 2007
Received in revised form 6 March 2008
Available online 22 April 2008

Keywords:
Composite materials
Modeling
Transverse cracking
Damage mechanics
Multiple damage modes

ABSTRACT

This paper presents a synergistic methodology to analyze damage behavior in composite laminates with transverse matrix cracks in plies of multiple orientations. The approach combines the strengths of micro-damage mechanics (MDM) and continuum damage mechanics (CDM) in predicting the stiffness degradation due to presence of transverse cracks. The micromechanics is performed on a representative unit cell using a three-dimensional finite element analysis to calculate the crack opening displacement (COD) accounting for the influence of the surrounding plies, the so-called constraint effect. This information is then incorporated in the CDM formulation dealing with laminates containing cracks in different ply orientations through a 'constraint parameter'. In CDM, a separate damage mode is defined for each type of crack and the expressions for engineering moduli of the damaged laminate are derived in terms of crack density and the constraint parameter. The COD and stiffness degradation predictions agree well with published experimental data for $[0/\pm\theta_4/0_{1/2}]_s$ laminate configuration. To enable damage analysis of other configurations of $[0_m/\pm\theta_n/0_{m/2}]_s$ laminate, a parametric study of the CODs is performed and using the computations a master equation is developed.

1. Introduction

In an un-constrained uni-directional composite, such as a ply not bonded to other plies, a uniform tensile stress applied normal to fibers will cause failure from a single crack lying in the matrix between fibers or at the fiber/matrix interface. However, if the composite is constrained, such as a ply within a laminate, then failure does not result from a single crack. Instead, multiple cracks form as the applied load increases. This phenomenon is described as multiple matrix cracking (Talreja, 2006). These matrix cracks usually form first in the ply thickness direction and then grow along fibers spanning the laminate width. Matrix cracks, usually the first mode of damage, are not critical from a final failure point of view but can lead to a significant reduction in individual ply properties as well as in the laminate properties. Modeling of stiffness degradation subsequent to matrix damage has been the topic of extensive research in the recent decades, especially for cross-ply laminates ($[0_m/90_n]_s$). A variety of analytical approaches have been suggested, e.g., ply-discount method, shear lag models (Highsmith and Reifsnider, 1982; Lim and Hong, 1989), variational method (Hashin, 1985), self-consistent approximation (Dvorak et al., 1985), 3-D laminate theory (Gudmundson and Ostlund, 1992) and continuum damage mechanics (Talreja, 1985a; Allen et al., 1987). However, most of the research work is limited to cross-ply laminates, which are easier to analyze but are not used often in practical applications. Analyzing damage in laminates of general layup is quite challenging due to multiplicity of damage modes and the constraints induced on individual ply cracks by the neighboring plies.

Composite laminates with off-axis plies are important for applications where structures undergo loading combinations that necessitate use of multiple fiber orientations to generate required properties. Still, damage in such laminates has not been fully analyzed. Masters and Reifsnider (1982) experimentally observed damage development in quasi-isotropic ($[0/\pm 45/90]_s$ and

* Corresponding author. Tel.: +1 979 845 1567; fax: +1 979 845 6051.
E-mail addresses: chandraveer@tamu.edu (C.V. Singh), talreja@aero.tamu.edu (R. Talreja).

0020-7683/$ - see front matter © 2008 Elsevier Ltd. All rights reserved.
doi:10.1016/j.ijsolstr.2008.04.004

$[0/90/\pm 45]_s$) carbon–epoxy laminates under fatigue loading. Tong et al. (1997a) conducted experimental investigations of matrix crack growth behavior under quasi-static and fatigue loadings in quasi-isotropic glass–epoxy laminates and used generalized plane-strain finite element analysis to predict stiffness degradation and ply stress distribution (Tong et al., 1997b). However, damage in off-axis plies is essentially a 3-D stress analysis problem and a generalized plane strain formulation cannot adequately address it. Other approaches such as equivalent constraint model (ECM), in combination with the first order shear deformation laminated plate theory (FSDT) (Zhang and Herrmann, 1999) and with a modified shear lag analysis (Kashtalyan and Soutis, 2000), have also been attempted. Recently, Yokozeki and Aoki (2004, 2005a,b) have analyzed laminates with obliquely crossed matrix cracks utilizing a two-dimensional shear lag analysis. Considering the complexity of the problem at hand, these works are good starting point but they provide approximate solutions whose accuracy cannot be fully verified as no exact analytical solutions currently exist.

To analyze the deformational response of composite laminates subsequent to matrix cracking, the most direct measure of crack influence over laminate properties is the "coefficient" of crack opening displacement (COD), i.e., average crack surface separation per unit of an applied load quantity. Only a few researchers in the past have focused on surface displacements of ply cracks in an explicit manner. Gudmundson and Ostlund (1992) derived analytical expressions for average stiffness properties of cracked symmetric laminates in terms of COD. They assumed that the average COD for matrix cracks in a composite laminate of general layup could be approximated by the analytical solutions of an array of parallel cracks in an infinite homogeneous medium. However, this completely neglects the constraint effect on COD and evaluating the consequence of such approximation is therefore necessary either by experimental or computational means. To study COD, Varna et al. (1993) developed a device to experimentally measure COD in cross-ply laminates. A separate study (Varna et al., 1997) verified the accuracy of different analytical models for estimating COD in cross-ply laminates. Joffe et al. (2001) later used a FE plane stress model to evaluate the average COD dependence on the crack spacing and on the constraint of adjacent sub-laminates.

The classical CDM approach is quite efficient in predicting stiffness degradation if certain phenomenological constants can be evaluated (Talreja, 1985b). An experimental evaluation of the constants may not be easy in all cases and to alleviate this limitation, Talreja (1996) later proposed a synergistic damage mechanics (SDM) approach and illustrated it to describe the deformational response of $[\pm\theta/90_2]_s$ laminates. This approach combines micromechanics and continuum damage mechanics judiciously to produce a versatile methodology. The micromechanical damage mechanics, or briefly, micro-damage mechanics (MDM) performs analysis of local stress-redistributions due to cracking, incorporating the micro-level geometry. On the other hand, CDM, as formulated by Talreja (1985a, 1991), allows a specific output of MDM (COD) to be used within a representative volume element (RVE), i.e., at meso level. In this way, the synergism between micromechanics and CDM effectively treats the multi-scale nature of damage. More recently, the SDM approach has also been extended to analyze viscoelastic behavior of composites with damage (Varna et al., 2004).

In the present study, we present a synergistic methodology to deal with matrix cracks in plies with multiple off-axis orientations. The continuum damage mechanics formulation of particular relevance to this work is the one presented by Talreja (1991, 1994), wherein the damage state in the laminate is described by second order tensors. In the present scenario, the damage state can be suitably represented by damage mode tensors regarding ply cracking in each orientation as an individual damage mode. The constraint effects on the cracked plies imposed by the surrounding plies are evaluated in terms of the COD changes in off-axis plies. CODs are determined using 3-D FE analysis and then subsequently used in the CDM model through the constraint parameter to predict the stiffness properties of the degraded laminate. The CODs are evaluated at different applied strains and the variation in these is checked against the experimental values at 0.4% and 0.6% strains. The strength of SDM approach lies in accurate COD calculation using computational micromechanics and an accurate damage description using CDM. Thus, SDM promises to be a pragmatic solution to the damage analysis problem for laminates with complex layups for which analytical results are difficult to derive. In order to make the SDM approach more versatile, detailed parametric studies are conducted to study the variables which may affect the constraint of un-cracked plies over cracked plies. Using these parametric studies, a master equation for CODs in terms of geometry and material variables is proposed. Also, the profile of average crack surface displacements through thickness of the cracked ply is studied for different laminate configurations. Finally, stiffness moduli for $[0_m/\pm\theta_n/0_{m/2}]_s$ laminates are predicted for different stiffness and thicknesses of cracked and supporting plies.

2. Synergistic damage mechanics methodology for $[\mathbf{0_m/\pm\theta_n/0_{m/2}}]_\mathbf{s}$ laminates

Consider a symmetric laminate with a general layup, e.g. $[0_m/\pm\theta_n/\phi_p]_s$, loaded in axial tension, with ϕ restricted to angles which do not cause cracking. The loading will produce an in-plane stress state in each off-axis ply consisting of normal stresses along and perpendicular to fibers in that ply and a shear stress in the plane of the ply. Depending on the values of θ, ϕ and ply properties, the stress perpendicular to the fibers could be tensile or compressive. Thus, on loading, an off-axis ply may or may not develop intralaminar cracks. When $\theta = 90^\circ$ the matrix will undergo multiple cracking in the transverse plies. For other cases of off-axis ply orientations, multiple cracking is typically observed to occur for angles from 50° to 90°. However, it has been observed that even in cases where these cracks do not initiate in the off-axis plies, the laminate moduli change with the applied load due to shear stress induced damage within the plies (Varna et al., 1999b).

When cracks are formed, the opening and sliding of crack surfaces alter the stress and strain states in the cracked plies, thereby changing the global deformational response of the laminate. The damage state in the laminate representative

volume element (RVE) can be described suitably by a set of second order tensors (Talreja, 1991, 1994). For $[0_m/\pm\theta_n/\phi_p]_s$ laminates with cracks in $+\theta_n$ and $-\theta_n$ plies, the damage state can be represented by two damage mode tensors, one each for matrix cracking in $+\theta_n$ plies and $-\theta_n$ plies. Following Talreja (1991, 1994), the elements of the damage tensor for a particular damage mode α can be expressed as

$$D_{ij}^{(\alpha)} = \frac{\kappa t_c^2}{st\sin\theta} n_i n_j \tag{1}$$

where $n_i = (\sin\theta, \cos\theta, 0)$ are components of the unit vector normal to a matrix crack plane in the off-axis ply in the global coordinate system X_i, i=1,2,3 and κ, known as the constraint parameter, represents the constraint effects of surrounding plies on the cracked plies. Fig. 1 shows a RVE illustrating one set of intralaminar cracks in an off-axis ply of a composite laminate. Although for clarity of illustration the cracking is shown only in one lamina, it is understood that in general it exists in multiple plies of the laminate. The thickness of the cracked plies is denoted by t_c, s is the crack spacing, t is the total laminate thickness, and W and L stand for the width and the length, respectively, of the RVE. For an initially orthotropic laminate with multiple damage modes, whose interactions are neglected, the stiffness matrix is given by Talreja (1991, 1994).

$$C_{pq} = C_{pq}^0 + \sum_{\alpha} C_{pq}^{(\alpha)} \tag{2}$$

where, $p, q = 1, 2, 6$, C_{pq}^0 is the stiffness coefficient matrix of the virgin laminate and $\Delta C_{pq} = \sum_\alpha C_{pq}^{(\alpha)} = C_{pq} - C_{pq}^0$ represents the stiffness change due to matrix cracking averaged (homogenized) over the RVE. As is shown in an earlier work (Talreja, 1985a), any two symmetrically placed damage fields of equal intensity in an initially orthotropic material will retain the orthotropic symmetry of the elasticity tensor. For $[0_m/\pm\theta_n/\phi_p]_s$ laminate configuration under axial loading, this condition is approximately met when $\phi = 0$ and $p = m/2$. For this case, we have

$$C_{pq}^0 = \begin{bmatrix} \frac{E_1^0}{1-\nu_{12}^0\nu_{21}^0} & \frac{\nu_{12}^0 E_2^0}{1-\nu_{12}^0\nu_{21}^0} & 0 \\ \frac{\nu_{12}^0 E_2^0}{1-\nu_{12}^0\nu_{21}^0} & \frac{E_2^0}{1-\nu_{12}^0\nu_{21}^0} & 0 \\ 0 & 0 & G_{12}^0 \end{bmatrix} \tag{3}$$

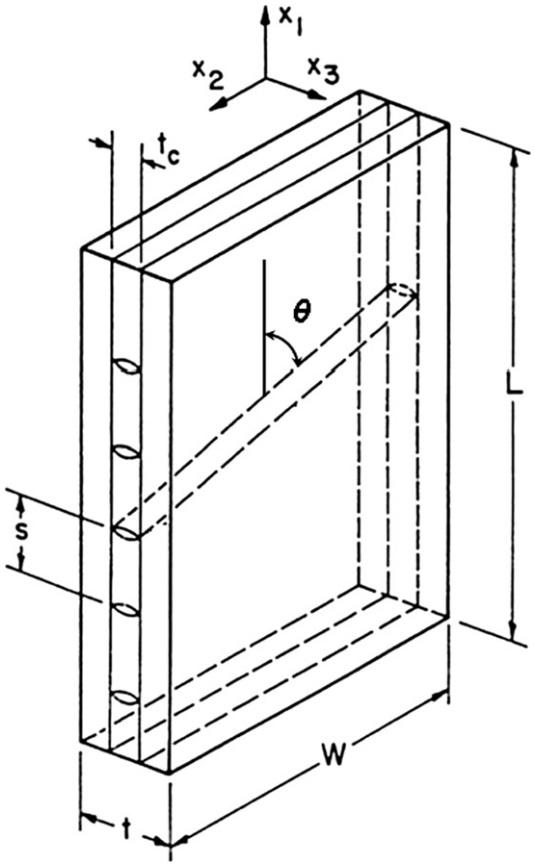

Fig. 1. A representative volume element (RVE) illustrating intralaminar multiple cracking in a general off-axis ply of a composite laminate.

$$\Delta C_{pq}(\pm\theta) = \Delta C_{pq}(+\theta) + \Delta C_{pq}(-\theta) = \frac{\kappa_\theta t_c^2}{st}\sin\theta \begin{bmatrix} 2a_1(\theta) & a_4(\theta) & 0 \\ & 2a_2(\theta) & 0 \\ \text{Symm} & & 2a_3(\theta) \end{bmatrix} \tag{4}$$

where, E_1^0, E_2^0, ν_{12}^0 and ν_{21}^0 are longitudinal modulus, transverse modulus, major and minor Poisson's ratio, respectively, for the virgin laminate. In Eq. (4), κ_θ is the constraint parameter and $a_i(\theta)$, i=1, 2, 3, 4 are phenomenological constants for ply of orientation θ. From this equation it is clear that the two symmetric damage modes ($+\theta$ and $-\theta$ cracking) effectively act as a single damage mode. The engineering moduli for the damaged laminate can now be derived from the following relationships:

$$E_1 = \frac{C_{11}C_{22} - C_{12}^2}{C_{22}}; \quad E_2 = \frac{C_{11}C_{22} - C_{12}^2}{C_{11}}; \quad \nu_{12} = \frac{C_{12}}{C_{22}}; \quad G_{12} = C_{66} \tag{5}$$

Thus, using Eqs. (2)–(5), we get

$$E_1(\theta) = \frac{E_1^0}{1-\nu_{12}^0\nu_{21}^0} + 2\frac{\kappa_\theta t_c^2 \sin\theta}{st}a_1(\theta) - \frac{\left[\dfrac{\nu_{12}^0 E_2^0}{1-\nu_{12}^0\nu_{21}^0} + \dfrac{\kappa_\theta t_c^2\sin\theta}{st}a_4(\theta)\right]^2}{\dfrac{E_2^0}{1-\nu_{12}^0\nu_{21}^0} + 2\dfrac{\kappa_\theta t_c^2\sin\theta}{st}a_2(\theta)} \tag{6}$$

$$E_2(\theta) = \frac{E_2^0}{1-\nu_{12}^0\nu_{21}^0} + 2\frac{\kappa_\theta t_c^2 \sin\theta}{st}a_2(\theta) - \frac{\left[\dfrac{\nu_{12}^0 E_2^0}{1-\nu_{12}^0\nu_{21}^0} + \dfrac{\kappa_\theta t_c^2\sin\theta}{st}a_4(\theta)\right]^2}{\dfrac{E_1^0}{1-\nu_{12}^0\nu_{21}^0} + 2\dfrac{\kappa_\theta t_c^2\sin\theta}{st}a_1(\theta)} \tag{7}$$

$$\nu_{12}(\theta) = \frac{\dfrac{\nu_{12}^0 E_2^0}{1-\nu_{12}^0\nu_{21}^0} + \dfrac{\kappa_\theta t_c^2\sin\theta}{st}a_4(\theta)}{\dfrac{E_2^0}{1-\nu_{12}^0\nu_{21}^0} + 2\dfrac{\kappa_\theta t_c^2\sin\theta}{st}a_2(\theta)} \tag{8}$$

$$G_{12}(\theta) = G_{12}^0 + 2\frac{\kappa_\theta t_c^2\sin\theta}{st}a_3(\theta) \tag{9}$$

As seen from Eqs. (6)–(9), the shear modulus is uncoupled from the other three moduli and thus can be treated independently. The three material constants $\kappa_\theta a_1, \kappa_\theta a_2$ and $\kappa_\theta a_4$ are present in the first three coupled equations and can be evaluated for a selected reference laminate, e.g. a cross ply laminate ($\theta = 90^\circ$), by using data generated either experimentally or by an analytical or a computational model. The remaining constant $\kappa_\theta a_3$ associated with the shear modulus change can in principle also be obtained similarly. However, experimental data to determine shear modulus are usually difficult to obtain. The analytical or computational determination of the shear modulus for a cracked cross ply laminate would require setting up a boundary value problem different from that needed to determine the other moduli. We shall not treat the shear modulus here since the constraint parameter κ_θ can as well be studied by considering the other three elastic moduli.

The stiffness change in a given laminate subsequent to damage depends on how much the matrix cracks "open up" in response to the imposed loading. This opening is affected by the neighboring plies as they apply constraint on the deformation of the cracked plies. Consequently, the stiffness change in a given laminate can be expressed as a function of the constraint effect measured in an appropriate way. Here a reference laminate belonging to the class of laminates considered is selected and the relative constraint effect in the other laminates is expressed with respect to this laminate. The stiffness change as a function of crack density in the reference laminate ($\theta = 90^\circ$) is determined either from experiments or from numerical simulations (FE or micromechanics). Based on notions of fracture mechanics, the relative constraint effect is taken as the ratio of the COD in the off-axis ply to that of the same-sized transverse crack in the reference laminate.

For laminates of the $[0_m/\pm\theta_n/0_{m/2}]_s$ configurations, the material constants a_i are assumed to remain unaffected by the angle θ for a given ply material. From experimental observations on carbon/epoxy (Talreja, 1996) and glass/epoxy (Varna et al., 1999a) laminates, this assumption has been found to hold true. This is supposedly because the damage-associated constants are primarily determined by the constituent ply properties and are only weakly dependent on ply orientation. Of course, the influence of the ply orientation on the constraint imposed by surrounding plies over damaged plies is important and is suitably carried by the 'constraint parameter' through changes in COD. The procedure to evaluate a_1, a_2, a_4 and κ_θ will now be described. Using Eqs. (2)–(4) with $\theta = 90$ and $s = s_0$; we obtain

$$\begin{bmatrix} \frac{E_1^0}{1-\nu_{12}^0\nu_{21}^0} & \frac{\nu_{12}^0 E_2^0}{1-\nu_{12}^0\nu_{21}^0} & 0 \\ & \frac{E_2^0}{1-\nu_{12}^0\nu_{21}^0} & 0 \\ \text{Symm} & & G_{12}^0 \end{bmatrix} + \frac{\kappa_{90} t_c^2}{s_0 t}\begin{bmatrix} 2a_1 & a_4 & 0 \\ & 2a_2 & 0 \\ \text{Symm} & & 2a_3 \end{bmatrix} = \begin{bmatrix} \frac{E_1}{1-\nu_{12}\nu_{21}} & \frac{\nu_{12}E_2}{1-\nu_{12}\nu_{21}} & 0 \\ & \frac{E_2}{1-\nu_{12}\nu_{21}} & 0 \\ \text{Symm} & & G_{12} \end{bmatrix} \tag{10}$$

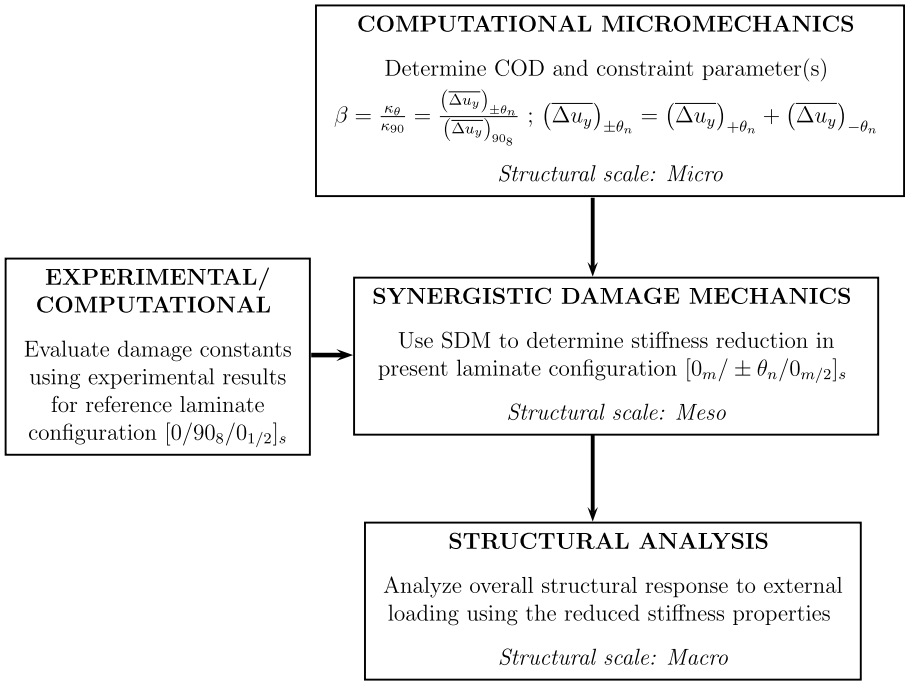

Fig. 2. Flowchart showing the multi-scale synergistic methodology for analyzing damage behavior in a class of symmetric laminates with layup $[0_m/\pm\theta_n/0_{m/2}]_s$ containing transverse cracks in $+\theta$ and $-\theta$ layers.

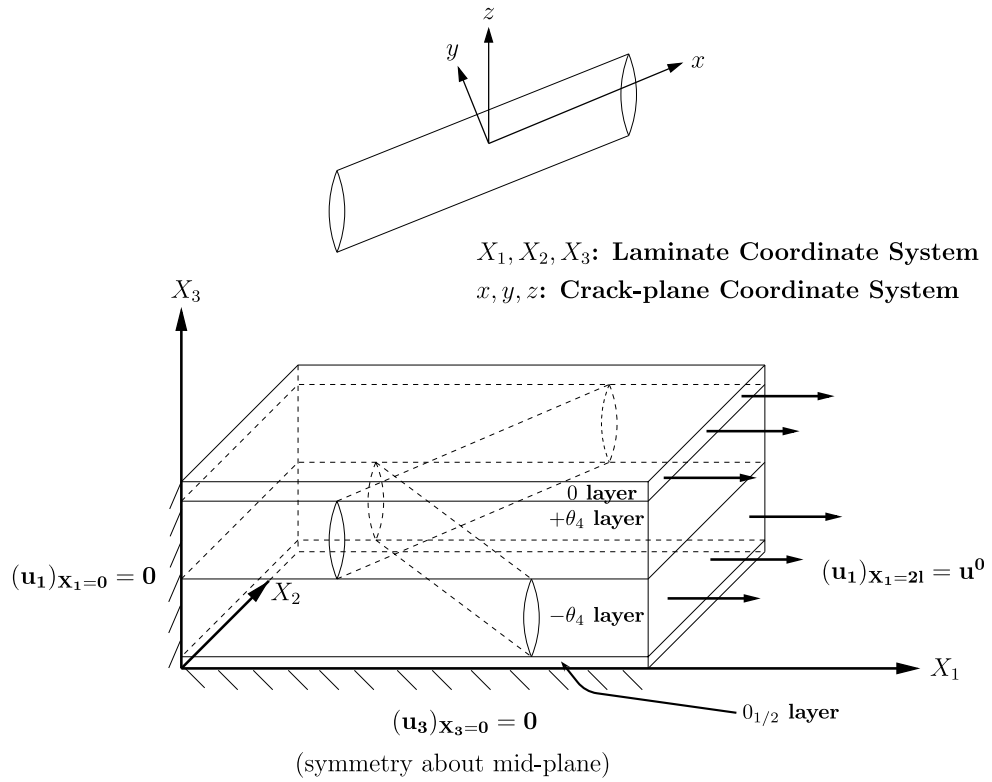

Fig. 3. A representative unit cell for FE analysis of $[0/\pm\theta_4/0_{1/2}]_s$ laminate.

where, the right-hand side of the equation represents the stiffness matrix of the damaged laminate expressed in terms of moduli $E_1, E_2, G_{12}, \nu_{12}$ and ν_{21} evaluated at crack density $s = s_0$. Solving this equation the material constants of interest can be written as

$$a_1\kappa_{90} = \frac{s_0 t}{2t_c^2}\left[\frac{E_1}{1-\nu_{12}\nu_{21}} - \frac{E_1^0}{1-\nu_{12}^0\nu_{21}^0}\right] \tag{11}$$

$$a_2\kappa_{90} = \frac{s_0 t}{2t_c^2}\left[\frac{E_2}{1-\nu_{12}\nu_{21}} - \frac{E_2^0}{1-\nu_{12}^0\nu_{21}^0}\right] \tag{12}$$

$$a_4\kappa_{90} = \frac{s_0 t}{t_c^2}\left[\frac{\nu_{12}E_1}{1-\nu_{12}\nu_{21}} - \frac{\nu_{12}^0E_1^0}{1-\nu_{12}^0\nu_{21}^0}\right] \tag{13}$$

The procedure for damage analysis in the synergistic damage mechanics approach is sketched in Fig. 2. As illustrated, this procedure combines micromechanics with CDM for complete evaluation of structural response. Micromechanics involves analysis to determine CODs in cracked plies within a RVE (or unit cell, if applicable), from which the constraint effect is evaluated, as we shall explain in the next section. The constraint effect is carried over in the CDM formulation through the constraint parameter. In a separate step, the damage constants $\kappa_{90}a_i$ are determined from data for a reference laminate, which, as mentioned earlier, is chosen here to be $[0/90_8/0_{1/2}]_s$. With the values of the $\kappa_{90}a_i$ constants and $\beta = \frac{\kappa_\theta}{\kappa_{90}}$ known, the CDM based expressions given by Eqs. (6)–(9)

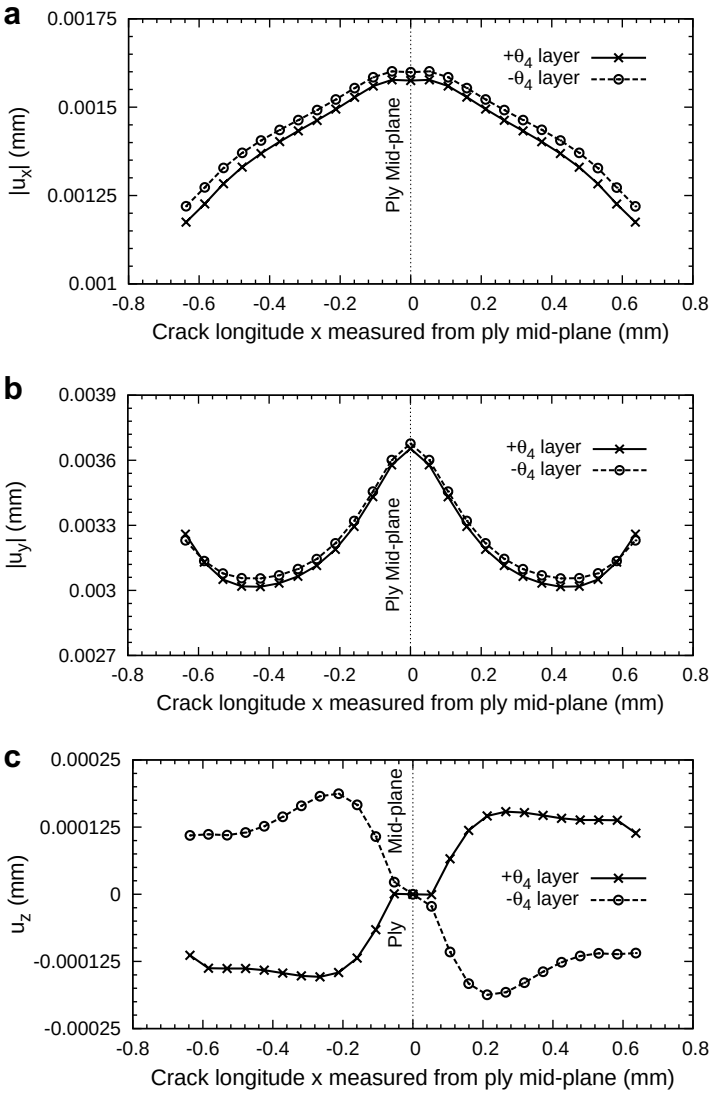

Fig. 4. Variation of average nodal displacements for $[0/\pm 70_4/0_{1/2}]_s$ laminate with respect to crack longitudinal (x) direction. The displacements u_x, u_y and u_z are averaged over cracked ply thickness.

are employed to predict stiffness degradation with crack density. The overall structural behavior is finally analyzed using the reduced stiffness properties for the laminate.

3. FE Modeling

Three-dimensional FE analysis is performed here as a micromechanical tool to evaluate the constraint effect. We note that although some analyses in literature use 2-D generalized FE models even for damage in off-axis plies, e.g. in $[0/90/\pm 45]_s$ laminates (Tong et al., 1997b), the boundary value problem necessitates a 3-D analysis. A representative geometric model for $[0/\pm\theta_4/0_{1/2}]_s$ laminate configuration along with the boundary conditions is shown in Fig. 3. As noted earlier, in this laminate configuration both sets of of-axis plies ($+\theta$ and $-\theta$ plies) experience almost identical constraint from the un-cracked 0-plies and hence the COD values for cracks in both orientations are expected to be nearly equal. The experimental results, which naturally show scatter, seem to support this (Varna et al., 1999b). We shall compute the CODs here to validate this expectation. Since the experimental data on COD were taken for cracks sufficiently away from neighboring cracks to eliminate the mutual crack interaction effect on CODs, focusing instead on the constraint effect, we shall simulate the experimental condition by choosing a large length of the RVE (unit cell) in the FE analysis conducted here.

For the laminate used in the experimental work, ply thickness and laminate width were equal to 0.125 and 3.5 mm, respectively. The ply material is glass–epoxy (HyE 9082Af, Fiberite) with in-plane properties $E_{11} = 44.7$ GPa, $E_{22} = 12.7$ GPa, $G_{12} = 5.8$ GPa and $\nu_{12} = 0.297$. To obtain the remaining properties for use in the 3-D model, the unidirectional ply is assumed transversely isotropic in the cross-sectional plane. Thus, $E_{33} = E_{22} = 12.7$ GPa; $G_{13} = G_{12} = 5.8$ GPa;$\nu_{13} = \nu_{12} = 0.297$; $G_{23} = \frac{E_{22}}{2(1+\nu_{23})} = 4.885$ GPa. The Poisson's ratio in the isotropic cross-sectional plane ν_{23} is taken as 0.3.

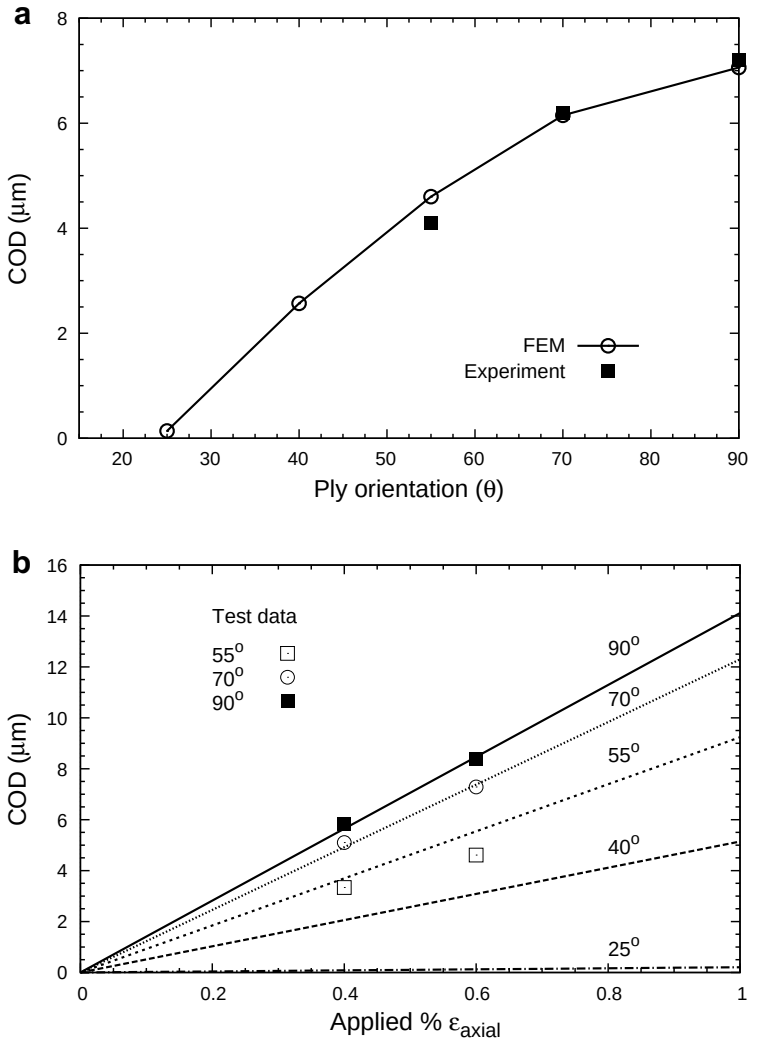

Fig. 5. Comparison of average CODs with experimental results (Varna et al., 1999b) for $[0/\pm\theta_4/0_{1/2}]_s$ laminate for (a) $\epsilon_{axial} = 0.5\%$ (b) varying ϵ_{axial}.

Separate 3-D FE models were constructed for $[0/\pm\theta_4/0_{1/2}]_s$ laminate configuration for ply orientations θ=25°, 40°, 55°, 70° and 90°. The mid-plane symmetry of the laminate was accounted for in the FE models. The matrix cracks were taken to have grown across the entire width of the specimen, as observed in the experimental work. ANSYS SOLID45 (eight-noded isoparametric) elements were used. Each FE model contained 20,000–60,000 elements. Mesh density was varied to arrive at an optimum level of accuracy and complexity of the 3-D FE model. Mapped meshing was utilized to flow the mesh smoothly through the thickness. Aspect ratio of elements near the crack surfaces was kept close to 1.0 for better accuracy. Linear Elastic FE analyses were carried out using ANSYS 9.0 at strain levels ranging from 0.1% to 1.0%. Displacement boundary conditions were applied by constraining the left end of the unit cell and providing required displacement at the right end, such that,

$$(u_1)_{X_1=0}=0;\quad (u_1)_{X_1=2l}=u^0;\quad (u_3)_{X_3=0}=0(\text{symmetry}) \tag{14}$$

where $\Delta X_1=2l$ and u^0 represent the length of unit cell and the applied displacement, respectively, in the laminate longitudinal direction.

4. Results and discussion

The results obtained by the SDM approach described in Section 2 are grouped in four sections below. First, the CODs computed by the FE model are compared with available experimental data to verify their accuracy. Next, the stiffness moduli for $[0/\pm\theta_4/0_{1/2}]_s$ laminates are predicted and compared with the experiments. A detailed parametric study is then conducted to determine the dependency of the COD on the factors that characterize the constraint effect. Finally, the constraint parameter is calculated from the COD results and used in the SDM methodology described above for prediction of stiffness property changes due to off-axis cracking in $[0_m/\pm\theta_n/0_{m/2}]_s$ laminates with varying m, n and stiffness ratio of the cracked plies relative to the constraining plies.

4.1. Crack surface displacements

Fig. 4 shows the variation of nodal displacements in x, y and z directions (see Fig. 3 for coordinate system) plotted with respect to x. All the displacements are averaged over thickness of the cracked layers. The average nodal displacements in x

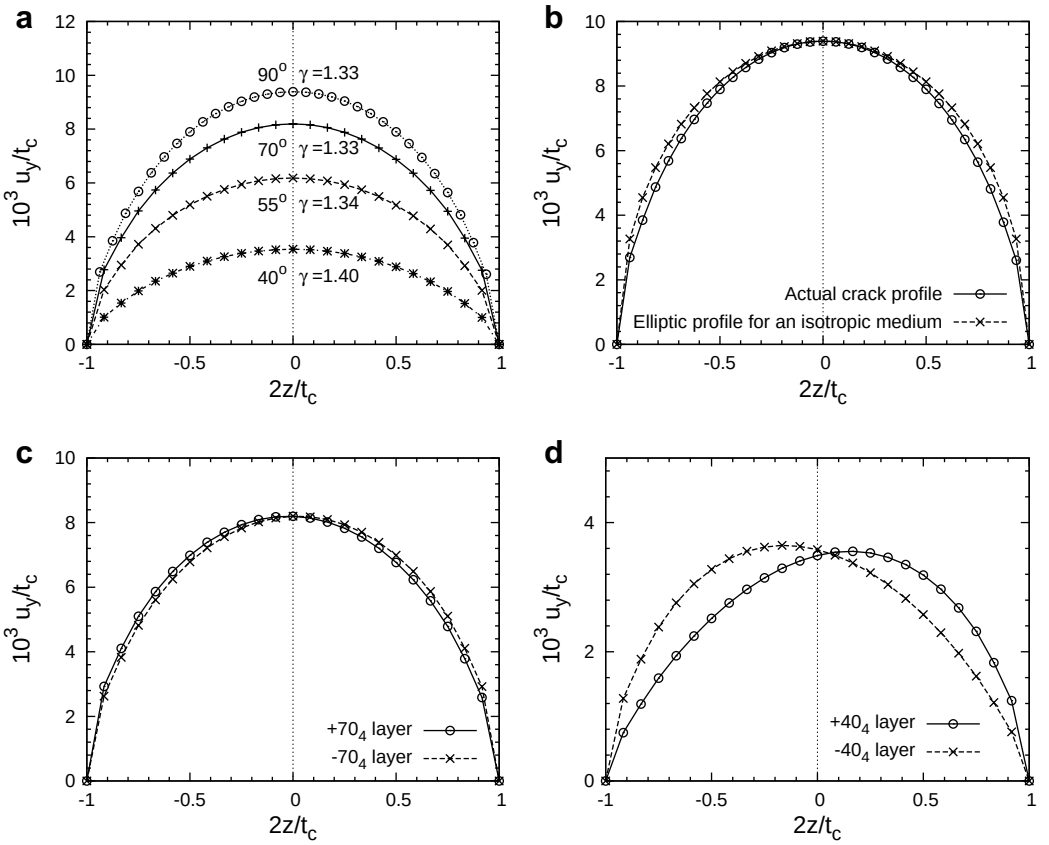

Fig. 6. COD profiles for cracked plies in $[0/\pm\theta_4/0_{1/2}]_s$ laminates. (a) CODs averaged over $-\theta$ and $+\theta$ plies; (b) Crack profile for 90° transverse crack compared with an elliptic profile for an isotropic medium; (c–d) COD profiles for $+\theta_4$ and $+\theta_4$ separately: (c) $\theta=70°$, (d) $\theta=40°$. The figures (c–d) depict the asymmetry of opening displacements for off-axis laminates, especially at a ply orientation farther from $\theta=90°$.

(crack longitudinal) and y (normal to crack plane) directions are nearly same in $+\theta$ and $-\theta$ layers in values and show similar trends over x; whereas in z-directions they are just opposite showing that as overall out of plane displacement is nullified. Thus, displacements averaged over the two orientations of cracks result in only symmetric components. The canceling of anti-symmetric components retains the overall orthotropic symmetry of the laminate. While the nodal displacements of the crack surfaces in y direction correspond to the opening mode (Mode I), the nodal displacements in x and z directions correspond, respectively, to the in-plane and out-of-plane sliding modes (Mode II and III). The sliding displacements are observed to be lower than the opening displacements. Especially, the out-of-plane displacements are negligible as compared to the opening displacements. Hence, for prediction of stiffness of the damaged laminate, crack opening displacements are enough. However, the in-plane sliding displacements may release substantial energy during fracture events and must be considered while analyzing the damage progression in off-axis laminates, which will be dealt in a future work.

In a previous work (Varna et al., 1999b), comprehensive experiments were carried out to evaluate CODs in $[0/\pm\theta_4/0_{1/2}]_s$ laminates subjected to tensile loading in axial direction. The full-size specimens (20 mm width) were loaded in an Instron 1272 testing machine to measure residual elastic properties at different states of damage and to characterize damage (density of cracks in the θ-plies) in the laminates at increasing tensile loads. Thin strips (3.5 mm width) were then cut longitudinally from the cracked specimens and were placed in a set-up developed for measuring COD. The set-up consisted of a miniature materials tester (MINIMAT) for loading the thin strip to open cracks, which were observed by an optical microscope equipped with a video camera. The video signal transmitted to a TV monitor displayed the crack profile at sufficient magnification ($\times$2463) to measure the COD. A typical COD of 10 μm was thus magnified to 24.63 mm. The micro-specimens (thin strips) were loaded at two pre-selected longitudinal strains, 0.4% and 0.6%, for the COD measurements. A specially constructed mini-extensometer was used to measure strains on the micro-specimens. These strains were much below the strains in the macro-specimens at which the intralaminar cracks were produced, thus generating no further cracking. The

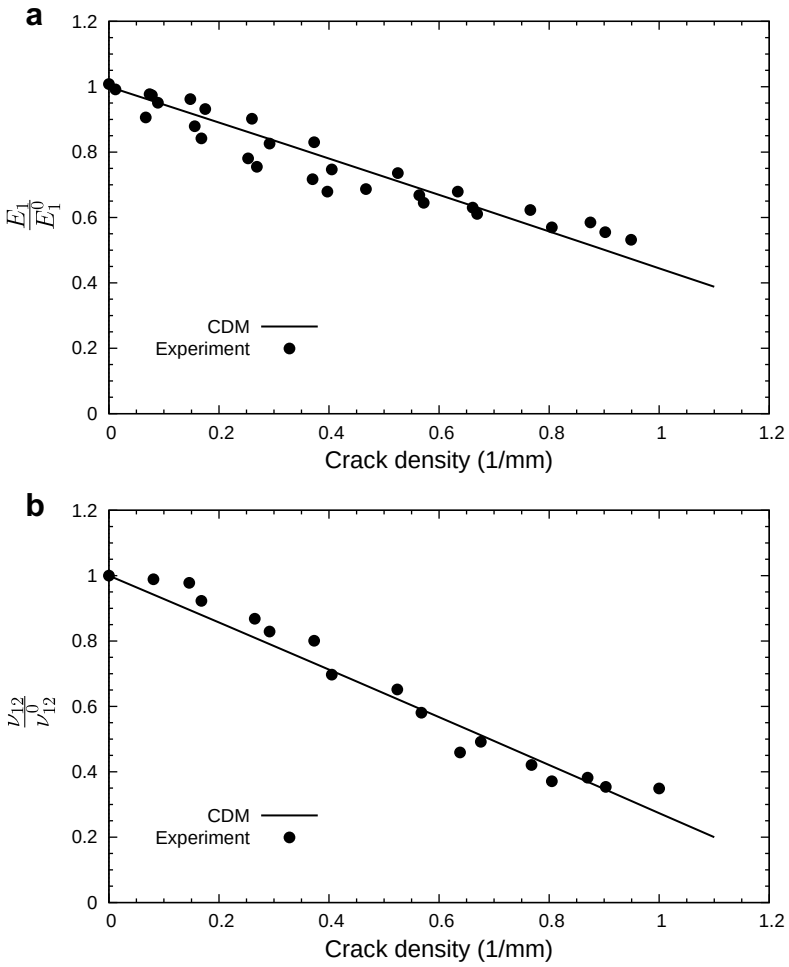

Fig. 7. Stiffness reduction for $[0/90_8/0_{1/2}]_s$ laminate compared with experimental results (Varna et al., 1999b). These results form the basis for computation of CDM constants.

CODs for a given crack were recorded at 25 equidistant points along the crack length (i.e. the total thickness of the ply group containing cracks).

In a general case, COD in a RVE depends on the crack spacing, the laminate layup parameters, the orientations of the cracked plies, their relative thickness as compared to the longitudinal plies, the imposed loading level and the ratio of stiffnesses of cracked and constraining plies. The average COD is defined as

$$\overline{\Delta u_y} = \frac{1}{t_c}\int_{-t_c/2}^{t_c/2} \Delta u_y(z)\mathrm{d}z \tag{15}$$

where Δu_y represents the separation of crack planes in the direction normal to the crack face. In experiments, no matrix cracks were observed on the specimen edge for ply orientations below $\theta = 40^\circ$. However, note that FE analysis assumes transverse cracks present for all angles of ply orientations. To estimate $\overline{\Delta u_y}$ numerically, Δu_y is determined from nodal y-direction displacements averaged over the entire crack surface. Furthermore, in keeping with the assumption of equal damage in $+\theta$ and $-\theta$ plies, the average COD values are averaged over the two orientations to eliminate any small differences. The experimental and numerically estimated results are compared in Fig. 5(a) for 0.5% axial strain. The experimental data for this strain is taken by averaging COD measurements for 0.4% and 0.6% axial strains. The variation of CODs with applied axial strain is compared with experimental data in Fig. 5(b).

The profiles of normalized CODs, averaged over $+\theta$ and $-\theta$ plies, through the thickness for different ply orientation are shown in Fig. 6(a). As expected, for cross-ply laminates, the profile is symmetric about mid-plane of the cracked ply and consequently the maximum COD occurs at the mid-plane of the cracked layer. This COD profile is different from an elliptic profile for a single crack in an infinite isotropic elastic medium subjected to a uniform far-field stress due to difference in constraint from the surrounding material. Fig. 6(b) compares the actual COD profile (based on FE computations) and an

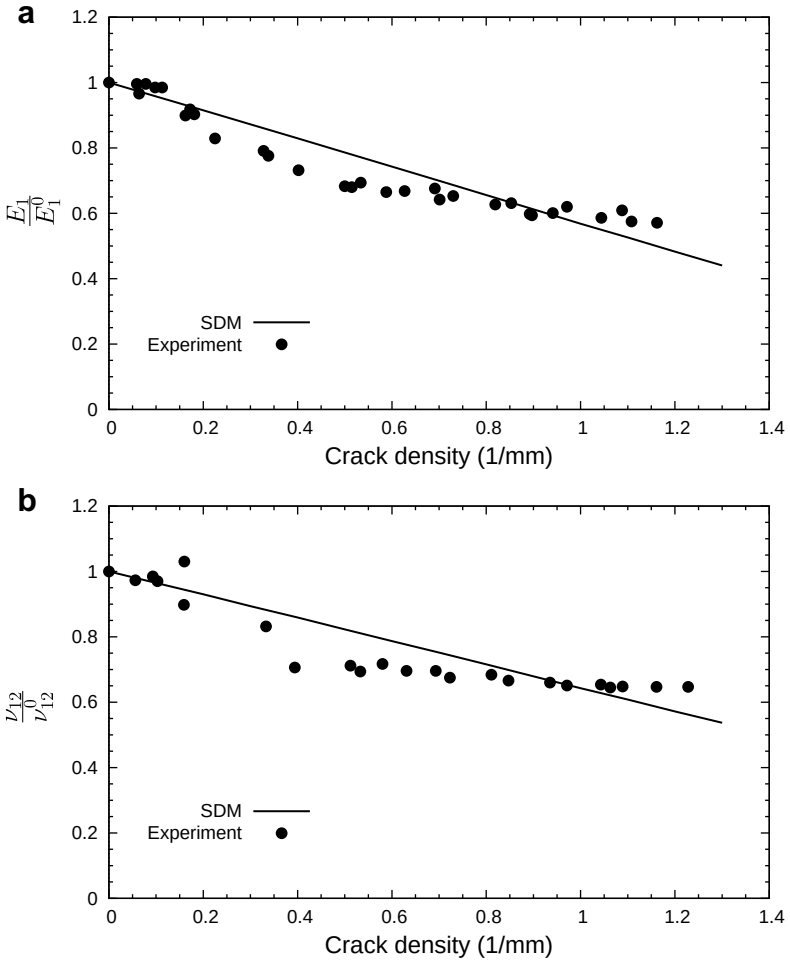

Fig. 8. Stiffness reduction for $[0/\pm 70_4/0_{1/2}]_s$ laminate compared with experimental results (Varna et al., 1999b).

elliptic profile with the same maximum COD. Thus, the magnitude of average COD for 90° crack is different from that for the elliptic crack. For other off-axis laminates, the crack surface displacements are not symmetric about the mid-plane as shown in Fig. 6(b)–(d). This asymmetry increases as we go away from cross-ply laminates ($\theta = 90^\circ$) and maximum COD does not occur midway through the thickness of the cracked $+\theta_4$ or $-\theta_4$ layers (e.g., for $\theta = 40^\circ$, see Fig. 6(d)). The aspect ratio of COD profiles, $\gamma = \frac{(\Delta u_y)_{\max}}{\overline{\Delta u_y}}$ varies from 1.33 for $\theta = 90^\circ$ to 1.40 for $\theta = 40^\circ$. This is different from the aspect ratio of 1.273 for an elliptic profile.

4.2. Prediction of stiffness degradation

In this section we will implement the SDM methodology described above for $[0/\pm\theta_4/0_{1/2}]_s$ laminates. Following the procedure sketched in Fig. 2, the constraint parameter κ_θ normalized by κ_{90} is taken as the average COD of the θ-cracks relative to the average COD of 90°-cracks. Thus,

$$\beta = \frac{\kappa_\theta}{\kappa_{90}} = \frac{(\overline{\Delta u_y})_{\pm\theta_4}}{(\overline{\Delta u_y})_{90_8}} \tag{16}$$

It is noted that the COD value in the numerator is the sum of CODs of the $+\theta_4$ and $-\theta_4$ cracks, while the COD in the denominator is of an 8-ply thick 90°-crack. All CODs are calculated at the same imposed displacement on the unit cells.

The procedure for stiffness prediction is now carried out in the following steps:

1. Determine the three material constants $\kappa_{90}a_1$, $\kappa_{90}a_2$ and $\kappa_{90}a_4$ by solving the three coupled Eqs. (11)–(13). The data needed to solve these equations are the elastic moduli E_1, E_2 $(= E_2^0)$ and ν_{12} (ν_{21} is given by the reciprocal relationship for orthotropic laminates) for a selected crack spacing $s = s_0$ in addition to the already known initial moduli and lamina

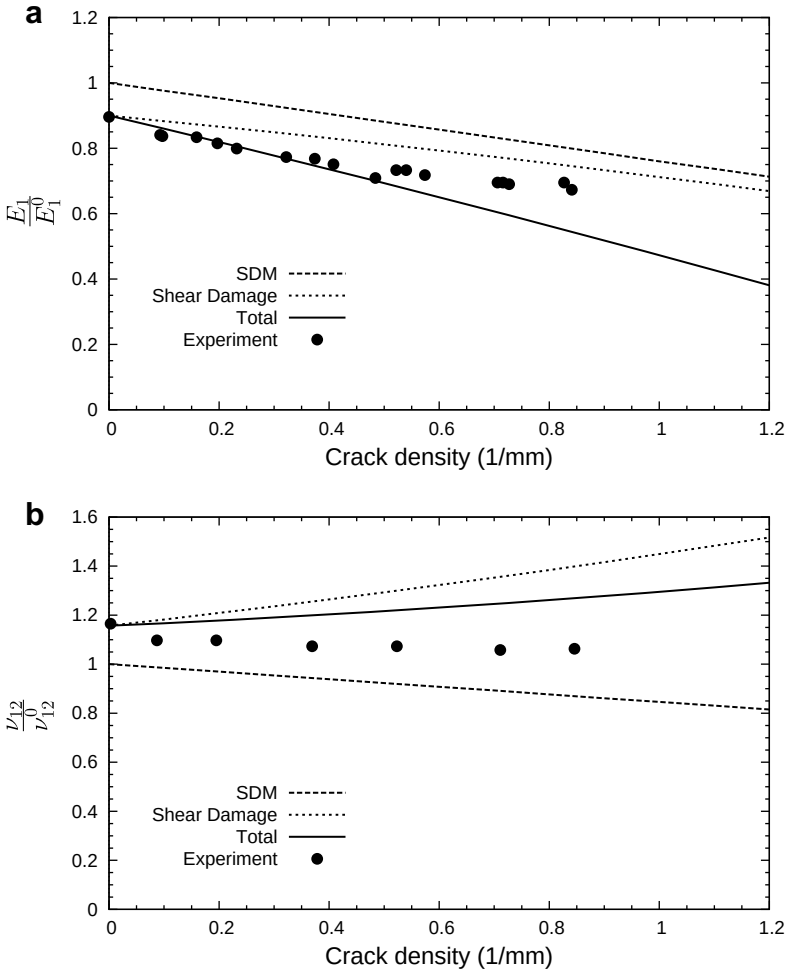

Fig. 9. Stiffness reduction for $[0/\pm 55_4/0_{1/2}]_s$ laminate compared with experimental results (Varna et al., 1999b).

thicknesses. This is the CDM procedure for cross ply laminates used in earlier works, e.g. (Talreja, 1991, 1994). The prediction of the two moduli E_1 and ν_{12} normalized with corresponding values for a virgin laminate are shown in Fig. 7 where they are compared with experimental data reported in Varna et al. (1999b).

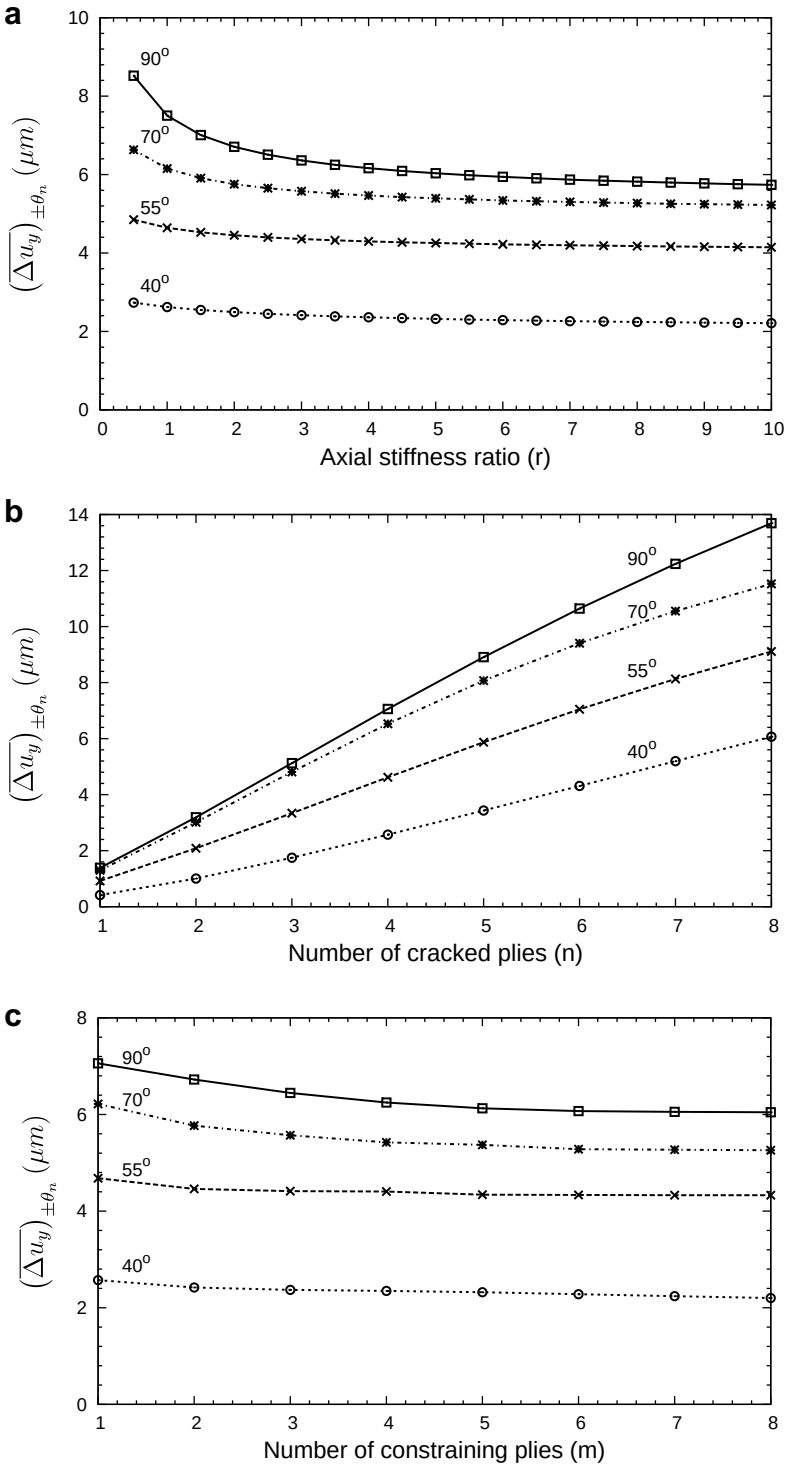

Fig. 10. Variation of average COD for $[0_m/\pm\theta_n/0_{m/2}]_s$ laminate with (a) axial stiffness ratio, r (for $m = 1, n = 4$); (b) number of cracked plies, n; and (c) number of constraining plies, m.

2. Determine β by using calculated COD values in Eq. (16). Find $\kappa_\theta a_1$, $\kappa_\theta a_2$ and $\kappa_\theta a_4$ by multiplying with β the constants $\kappa_{90} a_1$, $\kappa_{90} a_2$ and $\kappa_{90} a_4$ determined in Step 1. Calculate E_1, E_2 and ν_{12} from Eqs. (6)–(8) by substituting these constants, using the assumption that a_1, a_2 and a_4 are independent of θ, as noted above.

The elastic moduli E_1 and ν_{12} predicted by SDM approach are shown in Fig. 8 for $[0/\pm 70_4/0_{1/2}]_s$ laminate. Experimental data reported by Varna et al. (1999b) are also shown for comparison. The agreement with data is about the same as that obtained by using experimentally measured COD values in Eq. (16).

For the $[0/\pm 55_4/0_{1/2}]_s$ laminate the stiffness reduction is caused by matrix cracking as well as shear induced damage in off-axis plies, as discussed in Varna et al. (1999b), where a procedure for calculating stiffness reduction due to shear damage was described. Fig. 9 shows the predictions of E_1 and ν_{12} by the SDM procedure. Experimental data from Varna et al. (1999b) are also shown for comparison. The total reduction in the elastic moduli is taken as the sum of the two effects, as in Varna et al. (1999b), and the final values are shown in Fig. 9 along with experimental data. Once again, the agreement of predictions with the experimental data is nearly the same as that reported in Varna et al. (1999b) by using measured COD values.

It would be of interest to note that the stiffness predictions using experimentally measured COD values in Eq. (16) are subject to scatter, which is inherent in testing. Furthermore, the experimental procedure requires a specialized test set-up (Varna et al., 1993, 1999b), which is costly and takes a certain amount of training to operate. The 3-D FE computations on a unit cell, on the other hand, are easy to perform and can provide accurate values of CODs.

4.3. Parametric study of constraint effects

In the preceding section we have illustrated the SDM procedure for stiffness prediction of $[0/\pm\theta_4/0_{1/2}]_s$ laminates using computed average COD results, which provide the relative constraint parameter β (Eq. (16)). It is of interest to know how the

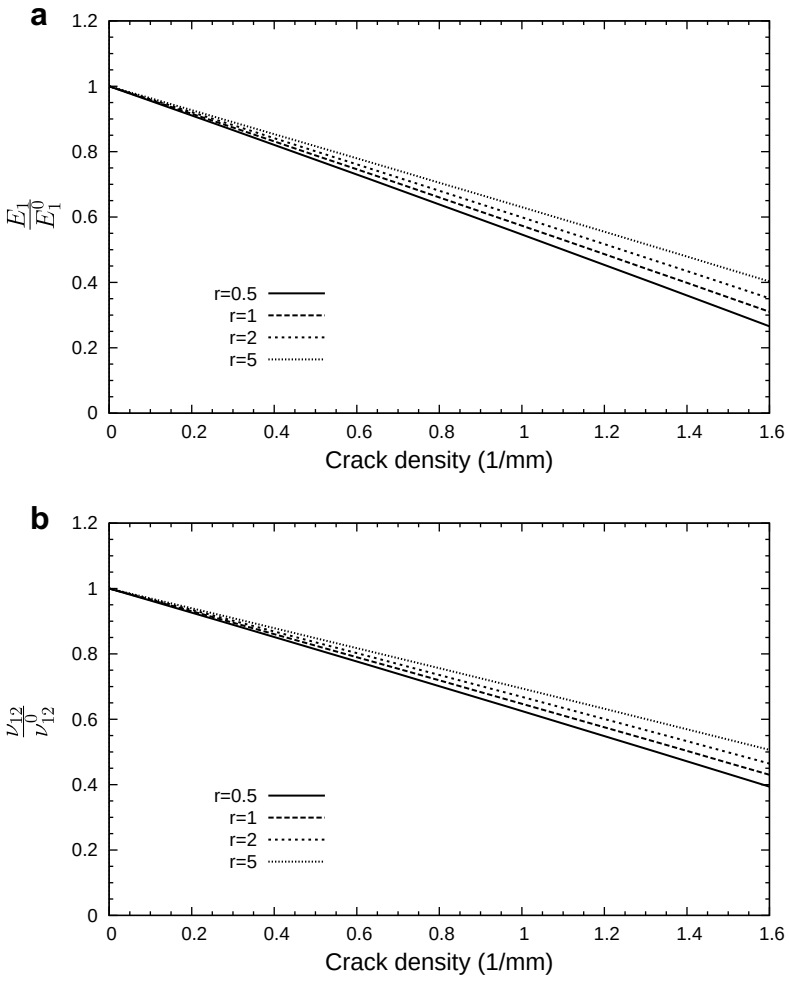

Fig. 11. Stiffness reduction for $[0/\pm 70_4/0_{1/2}]_s$ laminate for different axial stiffness ratio, r.

constraint parameter depends on the laminate configuration parameters within the broader class of laminates given by $[0_m/\pm\theta_n/0_{m/2}]_s$. This laminate configuration is restricted by the assumption that the cracks are present only in the $+\theta$ and $-\theta$ plies, which have nearly the same constraint. Thus, the parameters to vary are the crack orientation θ and ply thicknesses m and n. Furthermore, variation of the ply material itself can be accounted for through relative ply moduli, as suggested by previous studies (Joffe et al., 2001; Varna et al., 1999a).

The FE model described above was used to calculate COD values for various cases by systematically varying the parameters involved. First, the effect of relative stiffness of the plies was studied by fixing the ply thicknesses at $m = 1$ and $n = 4$ and varying θ in the range $40^\circ \leqslant \theta \leqslant 90^\circ$. Lower θ values were not used since the experimental observations suggest that cracks do not form at those ply orientations under axial tensile loading. The computed average COD values are plotted against a ply stiffness ratio in the laminate axial direction (X_1 direction) given by $r = \left(\frac{E_A^{\pm\theta}}{E_A^{90}}\right)$ in Fig. 10(a) for different θ-values. Here, $E_A^{\pm\theta}$ and E_A^{90} represent the axial stiffness of $\pm\theta$-plies and the 90°-plies, respectively.

Next the effect of cracked ply thickness, or equivalently, the number 'n' of adjacent cracked plies is studied by fixing $m = 1$. The average COD is plotted against n for different θ in Fig. 10(b). Finally, the effect of the thickness of the constraining plies is studied by fixing $n = 4$ and varying m. The COD variation for this case is shown in Fig. 10(c). All variations of average COD described above are captured in a master equation assuming that the individual effects are independent, i.e., non-interactive. Thus, the following equation results

$$(\overline{\Delta u_y})_{\pm\theta_n} = U \cdot f_1(\theta) \cdot f_2(r) \cdot f_3(m) \cdot f_4(n) \tag{17}$$

where, U is the average COD for the reference laminate $[0/90_8/0_{1/2}]_s$.

The parametric functions f_i are obtained by curve-fitting the computed data and are given by

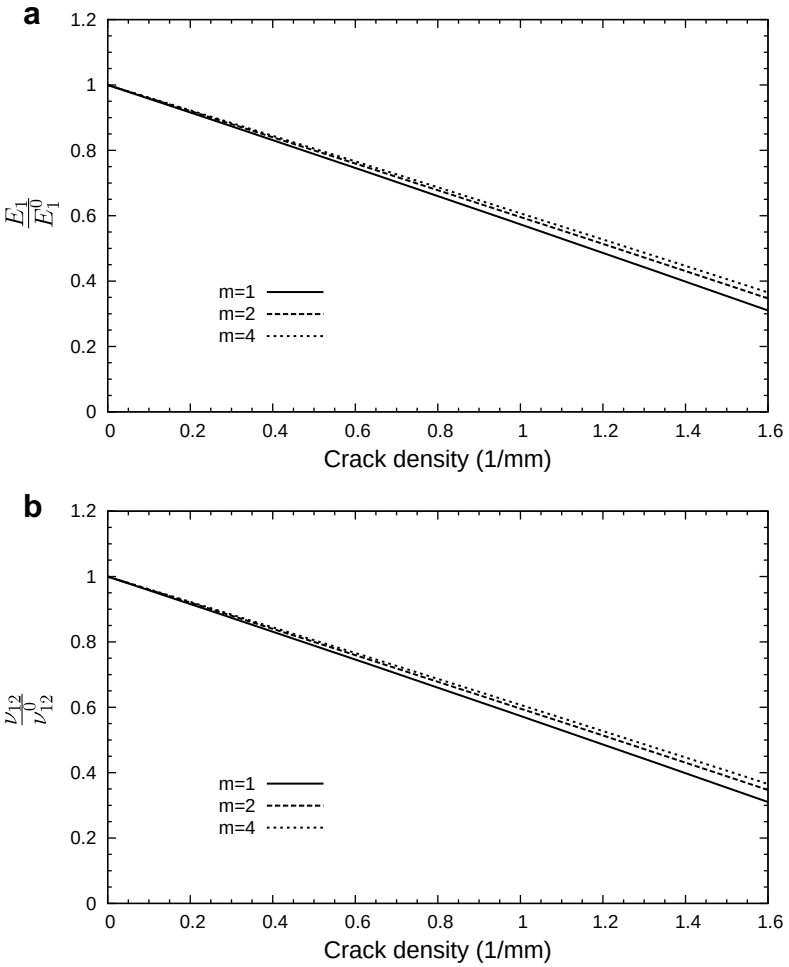

Fig. 12. Stiffness reduction for $[0_m/\pm 70_4/0_{m/2}]_s$ laminate for different number of constraining plies, m.

$$f_1(\theta) = \sin^2\theta \tag{18}$$

$$f_2(r) = r^{-c_1} \tag{19}$$

$$f_3(m) = \frac{c_2}{m} + c_3 \tag{20}$$

$$f_4(n) = c_4 n^{c_5} \tag{21}$$

The values of the constants appearing in these relations are found to be: $c_1 = 0.0871; c_2 = 0.1038; c_3 = 0.8949; c_4 = 0.247; c_5 = 0.99$. It is noted that these constants are laminate material specific.

4.4. Stiffness predictions for other laminates

The parametric study described above enables us to predict stiffness degradation in off-axis laminates with different geometry and stiffness values. For example, one can consider a laminate with stiffer outer plies. The average COD used in Eq. (16) for different values of stiffness ratio can be computed using Eq. (17). The variation of engineering moduli E_1 and ν_{12} for different stiffness ratios (r) for $[0/\pm 70_4/0_{1/2}]_s$ laminate is shown in Fig. 11. As expected, stiffer outer plies cause less sever degradation in the moduli. In contrast to changing the stiffness of outer plies, one can vary the number of constraining (m) or cracked plies (n). The effect of number of supporting plies over change in stiffness moduli E_1 and ν_{12} of the $[0_m/\pm 70_4/0_{m/2}]_s$ laminate is shown in Fig. 12. The effect of number of cracked plies over change in stiffness moduli E_1 and ν_{12} of the $[0/\pm 70_n/0_{1/2}]_s$ laminate is shown in Fig. 13. Fig. 11–13 indicate that the cracking ply thickness, i.e., crack size, has significant effect on stiffness degradation, while the thickness of the constraining plies as well as the change in axial stiffness ratio r have small effect.

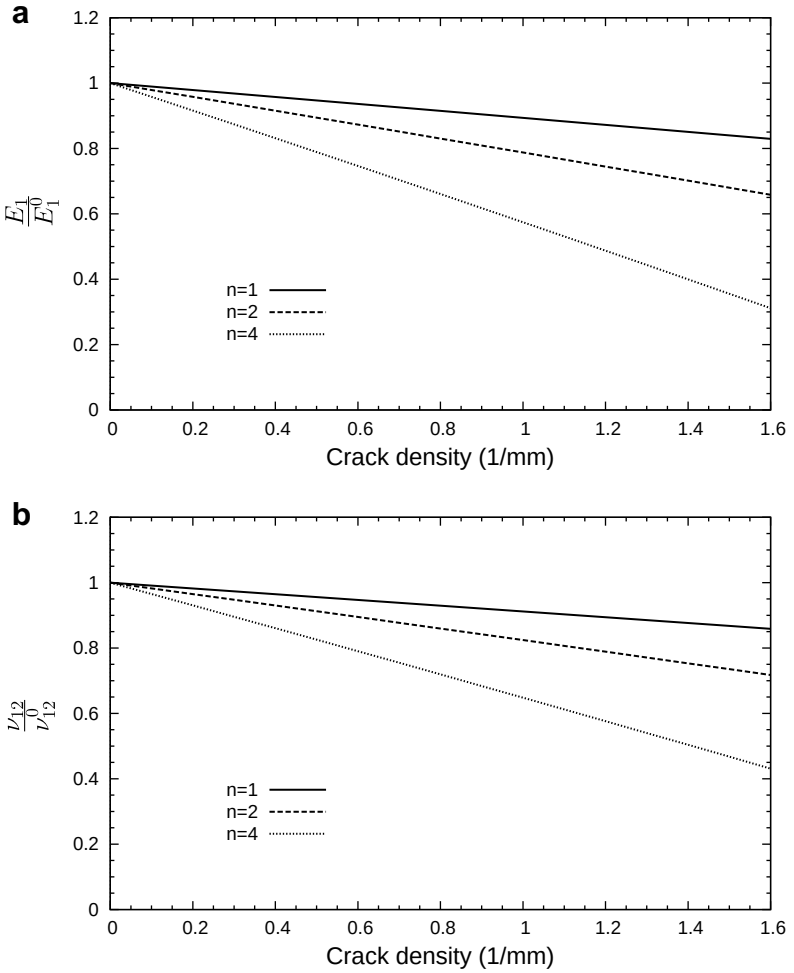

Fig. 13. Stiffness reduction for $[0/\pm 70_n/0_{1/2}]_s$ laminate for different number of cracked plies, n.

5. Conclusion

One major goal of damage mechanics is to provide methodologies for predicting changes in the mechanical response of composite laminates undergoing damage. It appears unrealistic at this point that this goal can be achieved for general laminates by a single method or approach. To make progress, however, it is necessary that the approach taken is capable of treating laminates of more complex configuration than the cross ply laminate, at the least. In the work reported here, we have made effort in this direction by considering a class of laminates given by $[0_m/\pm\theta_n/0_{m/2}]_s$. The approach taken has been to use the CDM framework that has the capabilities to treat general laminates with wide range of damage modes. To make the CDM framework versatile and practical, a methodology has been developed that utilizes computational micromechanics in sufficient measure to provide synergism with CDM, producing what we have called synergistic damage mechanics (SDM). Specifically, a constraint parameter (or function) is computed from a FE analysis of CODs in a unit cell and entered into the CDM stiffness-damage relationships. This provides a methodology for prediction of stiffness changes due to cracking in the off-axis plies when those changes for a selected reference laminate ($[0/90_8/0_{1/2}]_s$) are known.

Although the SDM approach was described in earlier works (Talreja, 1996; Varna et al., 1999b), it was illustrated only for one specific subclass of the general laminate configuration stated above, i.e. $[0/\pm\theta_4/0_{1/2}]_s$. Also, the CODs needed in the approach were measured on the edges of test coupons using a specialized set-up developed for the purpose. In the present work we have used those experimental CODs to verify the computed values by a 3-D FE analysis of appropriate unit cells. We have then performed a parametric study of CODs to cover the general $[0_m/\pm\theta_n/0_{m/2}]_s$ laminate over useful ranges of the parameters m, n and θ. A master equation is developed by curve-fitting the computed data that can provide the basis for stiffness prediction at a given damage state in the laminate at hand.

A successful completion of the task of treating two off-axis cracking modes ($+\theta$ and $+\theta$) points to proceeding further to treat three damage modes in $[0_m/\pm\theta_n/90_p]_s$. This will be the subject of our next report.

References

Allen, D.H., Harris, C.E., Groves, S.E., 1987. A thermomechanical constitutive theory for elastic composites with distributed damage. I. Theoretical development. Int. J. Solids Struct. 23 (9), 1301–1318.

Dvorak, G.J., Laws, N., Hejazi, M., 1985. Analysis of progressive matrix cracking in composite laminates. 1. Thermoelastic properties of a ply with cracks. J. Compos. Mater. 19 (3), 216–234.

Gudmundson, P., Ostlund, S., 1992. First order analysis of stiffness reduction due to matrix cracking. J. Compos. Mater. 26 (7), 1009–1030.

Hashin, Z., 1985. Analysis of cracked laminates: a variational approach. Mech. Mater. 4 (2), 121–136.

Highsmith, A., Reifsnider, K., 1982. Stiffness-reduction mechanisms in composite laminates. In: Reifsnider, K. (Ed.), Damage in Composite Materials. ASTM STP, pp. 103–117.

Joffe, R., Krasnikovs, A., Varna, J., 2001. COD-based simulation of transverse cracking and stiffness reduction in $[S/90_n]_s$ laminates. Comp. Sci. Tech. 61 (5), 637–656.

Kashtalyan, M., Soutis, C., 2000. Modelling stiffness degradation due to matrix cracking in angleply composite laminates. Plast. Rubber Compos. 29 (9), 482–488.

Lim, S., Hong, C., 1989. Prediction of transverse cracking and stiffness reduction in cross-ply laminate composites. J. Compos. Mater. 23 (7), 695–713.

Masters, J., Reifsnider, K., 1982. An investigation of cumulative damage development in quasi-isotropic graphite/epoxy laminates. In: Reifsnider, K. (Ed.), Damage in Composite Materials. ASTM STP, pp. 40–62.

Talreja, R., 1985a. A continuum mechanics characterization of damage in composite materials. Proc. Royal Soc. Lond. A 399 (1817), 195–216.

Talreja, R., 1985b. Transverse cracking and stiffness reduction in composite laminates. J. Compos. Mater. 19 (4), 355–375.

Talreja, R., 1991. Damage mechanics of composite materials based on thermodynamics with internal variables. In: Cardon, A., Verchery, G. (Eds.), Polymer Based Composite Systems for Structural Applications. Elsevier, London, pp. 65–79.

Talreja, R., 1994. Damage characterization by internal variables. In: Talreja, R. (Ed.), Damage Mechanics of Composite Materials. Elsevier, Amsterdam, pp. 53–78.

Talreja, R., 1996. A synergistic damage mechanics approach to durability of composite material systems. In: Cardon, A., Fukuda, H., Reifsnider, K. (Eds.), Progress in Durability Analysis of Composite Systems. A.A. Balkema, Rotterdam, pp. 117–129.

Talreja, R., 2006. Damage analysis for structural integrity and durability of composite materials. Fatigue Fract. Eng. Mater. Struct. 29 (7), 481–506.

Tong, J., Guild, F.J., Ogin, S.L., Smith, P.A., 1997a. On matrix crack growth in quasi-isotropic laminates – I. Experimental investigation. Comp. Sci. Tech. 57 (11), 1527–1535.

Tong, J., Guild, F.J., Ogin, S.L., Smith, P.A., 1997b. On matrix crack growth in quasi-isotropic laminates – II. Finite element analysis. Comp. Sci. Tech. 57 (11), 1537–1545.

Varna, J., Berglund, L., Talreja, R., Jakovics, A., 1993. A study of crack opening displacement of transverse cracks in cross-ply laminates. Int. J. Dam. Mech. 2 (3), 272–289.

Varna, J., Berglund, L., Krasnikovs, A., Chihalenko, A., 1997. Crack opening geometry in cracked composite laminates. Int. J. Dam. Mech. 6 (1), 96–118.

Varna, J., Akshantala, N.V., Talreja, R., 1999a. Crack opening displacement and the associated response of laminates with varying constraints. Int. J. Dam. Mech. 8 (2), 174–193.

Varna, J., Joffe, R., Akshantala, N.V., Talreja, R., 1999b. Damage in composite laminates with off-axis plies. Comp. Sci. Tech. 59 (14), 2139–2147.

Varna, J., Krasnikovs, A.I., Kumar, R.S., Talreja, R., 2004. A synergistic damage mechanics approach to viscoelastic response of cracked cross-ply laminates. Int. J. Dam. Mech. 13 (4), 301–334.

Yokozeki, T., Aoki, T., 2004. Stress analysis of symmetric laminates with obliquely crossed matrix cracks. Adv. Compos. Mater. 13, 121–140.

Yokozeki, T., Aoki, T., Ishikawa, T., 2005a. Consecutive matrix cracking in contiguous plies of composite laminates. Int J. Solids Struct. 42 (9-10), 2785–2802.

Yokozeki, T., Aoki, T., 2005b. Overall thermoelastic properties of symmetric laminates containing obliquely crossed matrix cracks. Compos. Sci. Tech. 65 (11-12), 1647–1654.

Zhang, J., Herrmann, K., 1999. Stiffness degradation induced by multilayer intralaminar cracking in composite laminates. Composites A 30 (5), 683–706.